HHS Public Access

Author manuscript

Nature. Author manuscript; available in PMC 2011 September 17.

Published in final edited form as:

Nature. 2011 March 17; 471(7338): 368–372. doi:10.1038/nature09857.

RIP3 mediates the embryonic lethality of caspase-8-deficient mice

William J. Kaiser[1], **Jason W. Upton**[1], **Alyssa B. Long**[2], **Devon Livingston-Rosanoff**[1], **Lisa P. Daley**[1], **Razqallah Hakem**[3], **Tamara Caspary**[2], and **Edward S. Mocarski**[1]

[1]Department of Microbiology and Immunology, Emory Vaccine Center, Emory University School of Medicine, Atlanta Georgia 30322

[2]Department of Human Genetics, Emory University, Atlanta, Georgia 30322

[3]Ontario Cancer Institute, University of Toronto, Toronto, Ontario, Canada M5G 2M9

Abstract

Apoptosis and necroptosis are complementary pathways controlled by common signaling adaptors, kinases and proteases; among these, caspase-8 (Casp8) is critical for death receptor (DR)-induced apoptosis. This caspase has also been implicated in nonapoptotic pathways that regulate Fas-associated via death domain (FADD)-dependent signaling and other less defined biological processes as diverse as innate immune signaling and myeloid or lymphoid differentiation patterns 1. Casp8 suppresses RIP3/RIP1 kinase complex-dependent 2–4 necroptosis 5 that follows DR-activation as well as a RIP3-dependent, RIP1-independent necrotic pathway that has emerged as a host defense mechanism against murine cytomegalovirus (MCMV) 6. Disruption of *Casp8* expression leads to embryonic lethality in mice between E10.5 and E11.5 7. Thus, Casp8 may naturally hold alternative RIP3-dependent death pathways in check in addition to its role promoting apoptosis. We find that RIP3 is responsible for the midgestational death of Casp8-deficient embryos. Remarkably, *Casp8*$^{-/-}$*Rip3*$^{-/-}$ double mutant mice are viable and mature into fertile adults with a full immune complement of myeloid and lymphoid cell types. These mice appear immunocompetent but develop lymphadenopathy by four months of age marked by accumulation of abnormal T cells in the periphery, a phenotype reminiscent of mice with Fas-deficiency (*lpr/lpr*). Casp8 contributes to homeostatic control in the adult immune system; however, RIP3 and Casp8 are together completely dispensable for mammalian development.

Correspondence to: William J. Kaiser, Department of Microbiology and Immunology, Emory Vaccine Center, 1462 Clifton Rd. NE, Emory University School of Medicine, Atlanta, Georgia 30322, Phone: 404-727-0563, Fax: 404-712-9736, wkaiser@emory.edu.

Author Contributions W.J.K., J.W.U., L.P.D., and D.L.R. designed and performed experiments and assembled figure panels. A.B.L. and T.C. guided evaluation of embryos. R.H. provided essential material support. E.S.M. supervised the project. W.J.K. and E.S.M. wrote the manuscript. T.C., R.H., J.W.U., L.P.D., and D.L.R. edited the text and figures during assembly of the manuscript.

Reprints and permissions information is available at www.nature.com/reprints

The authors declare no competing financial interests.

To determine whether Casp8 can hold RIP3 kinase-dependent death 2–5,8 in check, we employed murine L929 cells, a system that requires continued Casp8 expression for cell survival 9. Inhibition of Casp8 with either siRNA (Supplementary Fig. 1a) or zVAD-fmk (Supplementary Fig. 1c) induced death, as expected from prior studies 9. When treated with RIP3-specific shRNA, however, L929 cells were protected from death (Supplementary Fig. 1a), consistent with this being a RIP3-dependent necrotic death pathway. The MCMV M45 gene-encoded viral inhibitor of RIP activation (vIRA) blocks RIP3-dependent necrotic death 6. In keeping with the importance of a RIP3/RIP1 complex in necroptosis 2–4, vIRA blocked death whereas a tetra-alanine RHIM substitution mutant, M45*mut*RHIM 6 failed to suppress death induced by either Casp8 siRNA or zVAD (Supplementary Figs. 1b and d). Necrostatin-1 was employed to demonstrate that RIP1 kinase activity was necessary for necroptosis (Supplementary Fig. 1c). The specific viral inhibitor of Casp8 activation (vICA) encoded by the MCMV M36 gene 10 also induced this death pathway (Supplementary Fig. 1e and f). These data demonstrate that L929 cells succumb to RIP3-dependent necrotic death when Casp8 is inactive or eliminated.

Disruption of *Casp8* expression leads to embryonic lethality in mice between E10.5 and E11.5, coincident with embryonic vascular, cardiac and hematopoietic defects 7,11–13; however, the molecular mechanisms behind these defects remain poorly defined 7,11–13. To evaluate the potential contribution of RIP3 to embryonic lethality, we examined wild-type and *Casp8*$^{-/-}$ embryos as well as extra-embryonic tissues for *Rip3* expression. Based on *in situ* hybridization, *Rip3* transcript levels increased and tissue distribution broadened as embryonic development proceeded from E9.5 to E12.5 in both genotypes, indicating *Rip3* transcript is not regulated by *Casp8* (Fig. 1a and data not shown). At E9.5, *Rip3* was prominent in the apical ectodermal ridge (AER) of the hind-limb bud and the tail bud, and expanded to include the fore-limb bud AER, midline of the spinal cord, branchial arches and intersomitic regions by E10.5 through E12.5 (Fig. 1a, and data not shown), a signal that was absent from RIP3-deficient E10.5 embryos (Fig. 1b). Additionally, RIP3 was readily detected by immunoblot (IB) in E10.5 embryo and yolk sac cell lysates (data not shown). Mice homozygous for disruption of exons 3 and 4 in *Casp8* 14 died by E11.5 and presented with heart defects, hyperemia in the abdominal region, and undulation of the neural tube (Fig. 1c and Supplementary Fig. 2a) consistent with prior studies that used alternative targeting strategies to disrupt *Casp8* 7,11,13.

The yolk sac is the initial site of hematopoiesis prior to the transfer of function to intraembryonic sites. The most dramatic impact of *Casp8* disruption, either in embryonic tissues or in the yolk sac, is the disruption of endothelial cell organization leading to circulatory failure in the yolk sac, the likely culprit behind embryonic lethality 11,13. When we employed PECAM-specific antibody to localize endothelial cells in *Casp8*-deficient embryos (E10.5), we observed the expected contrast between an organized yolk sac vascular pattern in control mice and a disrupted pattern in *Casp8*-deficient mice (Fig. 1d). These observations affirmed the disruption of vascular development in *Casp8* null embryos. RIP3 was also detected in the yolk sac endothelium of both *Casp8*$^{+/-}$*Rip3*$^{+/-}$ and *Casp8*$^{-/-}$*Rip3*$^{+/-}$ embryos at this time (Supplementary Fig. 2b); thus, RIP3 was present in the cell populations most widely implicated in embryonic death of *Casp8*-deficient mice independent of *Casp8* expression. *Casp8* deficiency is also known to compromise primitive hematopoietic progenitor cell (HPC) development 7, a process dependent upon $CD41^+$ cells populating yolk sac blood islands and fetal sites 15. RIP3 was detected in $CD41^+$ cells in the yolk sac blood islands of embryos (Fig. 1e and Supplementary Fig. 2c). The striking $CD41^+$ cell fragmentation in the yolk sac blood islands of $Casp8^{-/-}Rip3^{+/-}$ embryos at E10.5 further implicates this kinase in processes leading to embryonic death.

To establish the role of the RIP3 kinase in embryonic lethality of *Casp8*-deficient mice, we generated double knock out (DKO) $Casp8^{-/-}Rip3^{-/-}$ embryos by a $Casp8^{+/-}Rip3^{+/-}$ intercross. In contrast to $Casp8^{-/-}Rip3^{+/-}$ embryos, which were developmentally arrested at ~E11.0, DKO embryos were indistinguishable from $Casp8^{+/-}Rip3^{-/-}$ or $Casp8^{+/-}Rip3^{+/-}$ embryos at E12.5 and later times, had a functioning heart and organized yolk sac endothelial architecture, and, remarkably, exhibited HPC colony formation at levels comparable to wild-type mice (Fig. 1f and g, Supplementary Fig. 2d and data not shown). The apparent normalization of the *Casp8*-deficient phenotype by removal of RIP3 suggested that this kinase was responsible for the ~E11.0 embryonic block, so we permitted the intercross pregnancies to complete gestation. PCR analysis performed on tissues from weanling mice confirmed deletion of *Casp8* exons 3–4 as well as deletion of *Rip3* in both alleles (Supplemental Fig. 3a). We detected RIP1, Casp8 and RIP3 in spleen and thymus from wild-type mice examined by IB (Fig. 2a). $Casp8^{+/+}Rip3^{-/-}$, $Casp8^{+/-}Rip3^{-/-}$, and DKO mice all lacked RIP3 but retained unaltered RIP1 levels in tissues. Casp8 was absent from DKO mice but present in other intercross progeny with predicted Mendelian frequencies (Fig. 2b). As expected, Casp8-deficient, RIP3-expressing progeny were not seen. Furthermore, when bred, adult DKO mice gave birth to viable mice that survived through adulthood and appeared similar to $Casp8^{+/-}Rip3^{-/-}$ mice bred in parallel (Supplementary Fig. 3b). Prior studies showed that conditional deletion of *Casp8* in epidermis promoted perinatal lethality characterized by chronic inflammation 16,17. DKO mice did not exhibit any evidence of skin inflammation when followed for more than six months, indicating that RIP3 must have played a proinflammatory role in the absence of epithelial Casp8 in prior studies. These results further indicate that embryonic lethality as well as a range of vascular degeneration and neural tube defects, together with hematopoietic abnormalities and chronic inflammation seen in mice lacking Casp8 are all RIP3-dependent.

To verify the functional elimination of *Casp8* in cells derived from DKO animals, we evaluated susceptibility to inducers of DR-mediated apoptosis. Although *Casp8* plays an essential role in macrophage differentiation 11, DKO mice produced $CD11b^+F4/80^+$ bone marrow-derived mononuclear (BMDM) cells just as readily as controls, and these cells lacked detectable RIP3 or Casp8 (Fig. 3a and b). Thus, the requirement for Casp8 during macrophage differentiation is suppressed by RIP3-deficiency. Macrophages prepared from wild-type, $Casp8^{+/+}Rip3^{-/-}$ and $Casp8^{+/-}Rip3^{-/-}$ mice died when exposed to reagents promoting Fas activation whereas DKO cells were completely resistant, consistent with the established role of this caspase in DR-induced apoptosis. In the presence of the caspase inhibitor zVAD-fmk, Fas activation promoted RIP3-dependent necroptosis in RIP3-containing BMDM cells (Fig. 3c). Furthermore, cells expressing RIP3 were susceptible to necroptosis, whereas *Rip3* knock-out and DKO mice remained resistant to this death pathway. Thus, DKO cells were insensitive to either extrinsic DR-induced apoptosis or RIP3-dependent necroptosis, consistent with their genotype. Previously, conditional knock-out of *Casp8* in the liver revealed its essential role in TNF or Fas-induced fatal hepatitis 11,18. DKO mice were resistant to anti-Fas-antibody treatment, survived for over 48 hours (Fig. 3d) and showed normal liver architecture (Fig. 3e), although they exhibited slightly elevated levels of the liver-associated transaminases ALT (alanine aminotransferase) and AST (aspartate aminotransferase) (data not shown). In contrast, $Casp8^{+/-}Rip3^{-/-}$ littermate control mice developed hepatitis (Fig. 3d and 3e). DKO mice were also resistant to administration of LPS in combination with the liver-specific transcriptional inhibitor D-(+) galactosamine (GalN), which induces a TNF-dependent fatal liver hepatitis in both wild-type 18 and $Casp8^{+/+}RIP3^{-/-}$ mice (Supplementary Fig. 4). This resistance was comparable to the negative control TRIF-deficient mice 19 (Supplementary Fig. 4).

Although RIP3 is dispensable for myeloid and lymphoid development 20, *Casp8* is essential for generation of both myeloid and lymphoid lineages 11,14,21,22. To determine whether this essential role of Casp8 was due to dysregulation of RIP3, we evaluated the characteristics of leukocytes from the thymus, bone marrow, spleen, and lymph node (LN) of DKO mice, littermate $Casp8^{+/-}Rip3^{-/-}$ and wild-type mice (Fig. 4a) by FACS analysis, detecting the presence of myeloid and lymphoid populations in all three genotypes based on forward (size) and side (granularity) light scatter properties (data not shown) in combination with surface markers. We observed inflammatory monocytes ($CD11b^{+}Ly6C^{hi}$) and polymorphonuclear leukocytes ($CD11b^{+}Ly6C^{int}$) in the bone marrow and spleen (Fig. 4a) of wild-type and DKO mice. Based on CD11c and F4/80 expression, dendritic cells and macrophages, respectively, populated the same tissues of DKO and $Casp8^{+/-}Rip3^{-/-}$ littermate controls (data not shown). Thus, myeloid cell populations continued to be generated in the absence of RIP3 and Casp8, consistent with the successful derivation of BMDM cells from DKO mice (see Fig. 3). NK ($CD49b^{+}CD3^{-}$), NKT ($CD49b^{+}CD3^{+}$) and B ($CD19^{+}$) lymphocytes, including predominant IgD^{+} as well as less prevalent IgD^{-} B cells (data not shown) were present in all tissues examined (Fig. 4a).

Defects in the Fas (CD95)-death receptor pathway promote the accumulation and expansion of lymphocytes and the development of autoimmune lymphoproliferative syndromes (ALPS) 23. Caspase-8 is downstream of Fas, and similarly DKO mice exhibited pronounced splenomegaly and lymphadenopathy over the first few months of age (Supplementary Fig. 5a, 5b, and 5c). Adult DKO mouse spleens ranged from three to seven times the size of $Casp8^{+/-}Rip3^{-/-}$ littermate controls (Fig. 4b and Supplementary Fig. 5b and 5c) and contained more lymphoid cells in splenic white pulp (data not shown). Histological examination revealed lymphocytic infiltrates in the salivary glands, pancreas, and lamina propria of both stomach and small intestine (data not shown). Consistent with size, DKO mice had significantly greater numbers of leukocytes in secondary lymphoid tissues such as spleen (Supplementary Fig. 5d) that appeared to result from abnormally high levels of $CD3^{+}$ T cells and to a lesser degree $CD19^{+}$ B cells (Supplementary Fig. 5e). Whereas these characteristics are consistent with the known role of Casp8 in DR-associated hematopoietic homeostasis 23, they contrast the characteristics of mice with Casp8 deficient T cells, where there are fewer T cells than B cells in secondary lymphoid tissues 14,22. Thus, there was a dramatic accumulation of T cells that contributed to lymphadenopathy and splenomegaly as DKO mice aged.

Casp8 deficient T cells exhibit defects in the response to antigens and mitogens 14,24. To compare T cell activation in DKO and *Casp8*$^{+/-}$*Rip3*$^{-/-}$ littermate controls, we evaluated the sensitivity of bulk splenocytes from mock and MCMV-infected mice, to anti-CD3 and anti-CD28 treatment. In contrast to prior observations on Casp8-deficient T cells 14,24, this treatment induced a response in mock-infected DKO cells and this response was enhanced at 7 days post MCMV infection. In fact, the CD8 T cells from DKO mice responded with an increased frequency in bifunctional INFγ^{+}TNF^{+} cells (Fig. 4c). Furthermore, DKO mice survived a dose of virus that is lethal to immunocompromised *scid/scid* mice and controlled viral replication levels for 30 days similar to *Casp8*$^{+/-}$*Rip3*$^{-/-}$ littermate controls (data not shown). Although more characterization is required to fully understand the quality of the immune response in DKO mice, T cell receptor-dependent activation of naïve and enhanced activation of antigen-exposed T cells is clearly retained despite the combined disruption of *Casp8* and *Rip3*.

Fas-deficient (*lpr/lpr*) mice are marked by the accumulation in the periphery of the CD3^{+} T cells that are B220^{+} but lack CD4 and CD8; these cells have been ascribed to a failure of apoptosis 25. DKO mice had normal CD4 and CD8 T cell populations in the thymus (Supplementary Fig. 5f), but contained this signature B220^{+} T cell population in secondary lymphoid organs (Fig. 4d and Supplementary Fig. 5g). Interestingly, conditional deletion of Casp8 in T cells, while resulting in lymphadenopathy did not result in the emergence of this signature phenotype 22, suggesting that RIP3-dependent necroptosis eliminates T cells where Casp8 is absent or nonfunctional. Thus, Fas DR-induced death pathways is essential for immune homeostasis and in the absence of both Casp8 and RIP3, excess unusual T cells likely accumulate due to a failure of both apoptosis and necroptosis.

The data presented here point to RIP3 as the vital target of Casp8 during mammalian development, with Casp8 functioning during embryogenesis to restrict RIP3 rather than to mediate apoptosis. We speculate that the RIP3-dependent pathway controlled by Casp8 during embryogenesis, as well as later in life, is related to known necrotic pathways controlled by this kinase. Eliminating this RIP3-dependent embryonic death in combination with Casp8-deficiency results in the accumulation of abnormal T cells starting in the first few months of age but does not lead to defects at other developmental stages. Casp8 may have other nonapoptotic roles such as influencing cell motility and proliferation; however one key role of Casp8 is its essential nonapoptotic function to control RIP3. FADD promotes Casp8 activation within the death-inducing signaling complex (DISC), a process subject to regulation by cFLIP. Deletion of FADD, cFLIP or Casp8 in all tissues causes a common pattern of vascular and hematopoietic defects associated with embryonic lethality in mice around E10.5 1, suggesting the coordinate control of RIP3 by these three players during development. The signals controlling activation of Casp8 and/or RIP3 during embryogenesis remain to be identified. Nevertheless, therapeutic strategies targeting DISC components aimed at apoptosis will need to take into account the likely triggering of RIP3-dependent pathways. Upon combined elimination of Casp8 and RIP3, defects in DR-dependent lymphocyte differentiation and homeostasis emerge. The discovery that Casp8 suppresses RIP3 pathways and is essential for maintenance of the vasculature, hematopoiesis, suppression of the innate immune system and T cell function points to the unexpected importance of these pathways in humans and other mammals. The observation here that Casp8 is a gatekeeper, suppressing RIP3 during development in addition to promoting apoptosis mediated via death receptors, promises to have broad implications in approaches to cancer therapy and regenerative medicine as well as during elaboration of the innate and adaptive phases of the immune response.

METHODS SUMMARY

RIP3$^{-/-}$20 and TRIF mutant (Strain - C57BL/6J-Ticam1^{Lps2}) 19 mice have been described previously. *Casp8*$^{+/-}$ mice were generated by crossing *Casp8*$^{fl3\text{-}4/wt}$ 14 with Rosa-CreER mice [26]. *Rip3*$^{-/-}$ and *Casp8*$^{+/-}$ mice were subsequently intercrossed. Embryos and yolk sacs were harvested from timed pregnancies at the indicated day post-coitus. Genotypes were determined by PCR from tail-snips or fetal tissue as described. Fatal hepatitis was induced by intraperitoneal injection with 12.5 μg of anti-mouse Fas antibody (clone Jo2, BD Biosciences). Tissue processing and staining was performed by Emory University Division of Animal Resources (EU-DAR). Mice were bred and maintained by EU-DAR where all procedures were approved by the Emory University Institutional Animal Care and Use Committee. Immunoblotting, preparation of protein extracts, and immunoprecipitations were as previously described [27]. Whole-mount *in situ* hybridization was performed as described [28], with digoxigenin-labeled antisense RNA probes transcribed from linearized RIP3 encoding plasmid (accession number BC029210, ATCC) according to the manufacturer's directions (Roche). Yolk sacs were fixed and stained for immunofluorescence microscopy by standard methods, and images were acquired on a Carl-Zeiss LSM 510 META confocal fluorescence microscope. Bone marrow derived macrophages were generated and viability determined as previously described 6. Cells for flow cytometry were harvested, processed and stained with indicated antibodies by standard methods. Data were acquired using an LSRII flow cytometer (BD Biosciences) and analyzed with FlowJo software.

Supplementary Material

Refer to Web version on PubMed Central for supplementary material.

Acknowledgements

We acknowledge Douglas Green, Andrew Oberst, and Christopher Dillon (St. Jude's Children's Research Hospital) for the kind provision of the essential materials and insightful discussions. We thank Vishva Dixit and Kim Newton (Genentech) for *RIP3*$^{-/-}$ mice, Andrew Kowalczyk, Rebecca Oas, Sam Speck, and Rafi Ahmed (Emory University) for providing reagents, Thomas Kaufmann (University of Bern) for technical advice, Cheryl Strauss (Emory University) for editing, and A. Louise McCormick (Emory University) for discussion and comments on the manuscript. Additionally, we appreciate Minida Dowdy and Jennifer Perry of the Division of Animal Resources at Emory University for mouse colony maintenance. Supported by N.I.H (PHS grants R01 AI20211 and AI30363 to E.S.M).

References

1. Strasser A, Jost PJ, Nagata S. The many roles of FAS receptor signaling in the immune system. Immunity. 2009; 30:180–192. [PubMed: 19239902]

2. Cho YS, et al. Phosphorylation-driven assembly of the RIP1-RIP3 complex regulates programmed necrosis and virus-induced inflammation. Cell. 2009; 137:1112–1123. [PubMed: 19524513]
3. He S, et al. Receptor interacting protein kinase-3 determines cellular necrotic response to TNF-alpha. Cell. 2009; 137:1100–1111. [PubMed: 19524512]
4. Zhang DW, et al. RIP3, an Energy Metabolism Regulator that Switches TNF-Induced Cell Death from Apoptosis to Necrosis. Science. 2009
5. Holler N, et al. Fas triggers an alternative, caspase-8-independent cell death pathway using the kinase RIP as effector molecule. Nat Immunol. 2000; 1:489–495. [PubMed: 11101870]
6. Upton JW, Kaiser WJ, Mocarski ES. Virus inhibition of RIP3-dependent necrosis. Cell Host Microbe. 2010; 7:302–313. [PubMed: 20413098]
7. Varfolomeev EE, et al. Targeted disruption of the mouse Caspase 8 gene ablates cell death induction by the TNF receptors, Fas/Apo1, and DR3 and is lethal prenatally. Immunity. 1998; 9:267–276. [PubMed: 9729047]
8. Chan FK, et al. A role for tumor necrosis factor receptor-2 and receptor-interacting protein in programmed necrosis and antiviral responses. J Biol Chem. 2003; 278:51613–51621. [PubMed: 14532286]
9. Yu L, et al. Regulation of an ATG7-beclin 1 program of autophagic cell death by caspase-8. Science. 2004; 304:1500–1502. [PubMed: 15131264]
10. McCormick AL, Skaletskaya A, Barry PA, Mocarski ES, Goldmacher VS. Differential function and expression of the viral inhibitor of caspase 8-induced apoptosis (vICA) and the viral mitochondria-localized inhibitor of apoptosis (vMIA) cell death suppressors conserved in primate and rodent cytomegaloviruses. Virology. 2003; 316:221–233. [PubMed: 14644605]
11. Kang TB, et al. Caspase-8 serves both apoptotic and nonapoptotic roles. J Immunol. 2004; 173:2976–2984. [PubMed: 15322156]
12. Kang TB, et al. Mutation of a self-processing site in caspase-8 compromises its apoptotic but not its nonapoptotic functions in bacterial artificial chromosome-transgenic mice. J Immunol. 2008; 181:2522–2532. [PubMed: 18684943]
13. Sakamaki K, et al. Ex vivo whole-embryo culture of caspase-8-deficient embryos normalize their aberrant phenotypes in the developing neural tube and heart. Cell Death Differ. 2002; 9:1196–1206. [PubMed: 12404118]
14. Salmena L, et al. Essential role for caspase 8 in T-cell homeostasis and T-cell-mediated immunity. Genes Dev. 2003; 17:883–895. [PubMed: 12654726]
15. Mitjavila-Garcia MT, et al. Expression of CD41 on hematopoietic progenitors derived from embryonic hematopoietic cells. Development. 2002; 129:2003–2013. [PubMed: 11934866]
16. Kovalenko A, et al. Caspase-8 deficiency in epidermal keratinocytes triggers an inflammatory skin disease. J Exp Med. 2009; 206:2161–2177. [PubMed: 19720838]
17. Lee P, et al. Dynamic expression of epidermal caspase 8 simulates a wound healing response. Nature. 2009; 458:519–523. [PubMed: 19204729]
18. Kaufmann T, et al. Fatal hepatitis mediated by tumor necrosis factor TNFalpha requires caspase-8 and involves the BH3-only proteins Bid and Bim. Immunity. 2009; 30:56–66. [PubMed: 19119023]
19. Hoebe K, et al. Identification of Lps2 as a key transducer of MyD88-independent TIR signalling. Nature. 2003; 424:743–748. [PubMed: 12872135]
20. Newton K, Sun X, Dixit VM. Kinase RIP3 is dispensable for normal NF-kappa Bs, signaling by the B-cell and T-cell receptors, tumor necrosis factor receptor 1, and Toll-like receptors 2 and 4. Mol Cell Biol. 2004; 24:1464–1469. [PubMed: 14749364]
21. Beisner DR, Ch'en IL, Kolla RV, Hoffmann A, Hedrick SM. Cutting edge: innate immunity conferred by B cells is regulated by caspase-8. J Immunol. 2005; 175:3469–3473. [PubMed: 16148088]
22. Salmena L, Hakem R. Caspase-8 deficiency in T cells leads to a lethal lymphoinfiltrative immune disorder. J Exp Med. 2005; 202:727–732. [PubMed: 16157684]
23. Bidere N, Su HC, Lenardo MJ. Genetic disorders of programmed cell death in the immune system. Annu Rev Immunol. 2006; 24:321–352. [PubMed: 16551252]

24. Ch'en IL, et al. Antigen-mediated T cell expansion regulated by parallel pathways of death. Proc Natl Acad Sci U S A. 2008; 105:17463–17468. [PubMed: 18981423]

25. Laouar Y, Ezine S. In vivo CD4+ lymph node T cells from lpr mice generate CD4-CD8- B220+TCR-beta low cells. J Immunol. 1994; 153:3948–3955. [PubMed: 7523511]

Author Manuscript
Author Manuscript
Author Manuscript

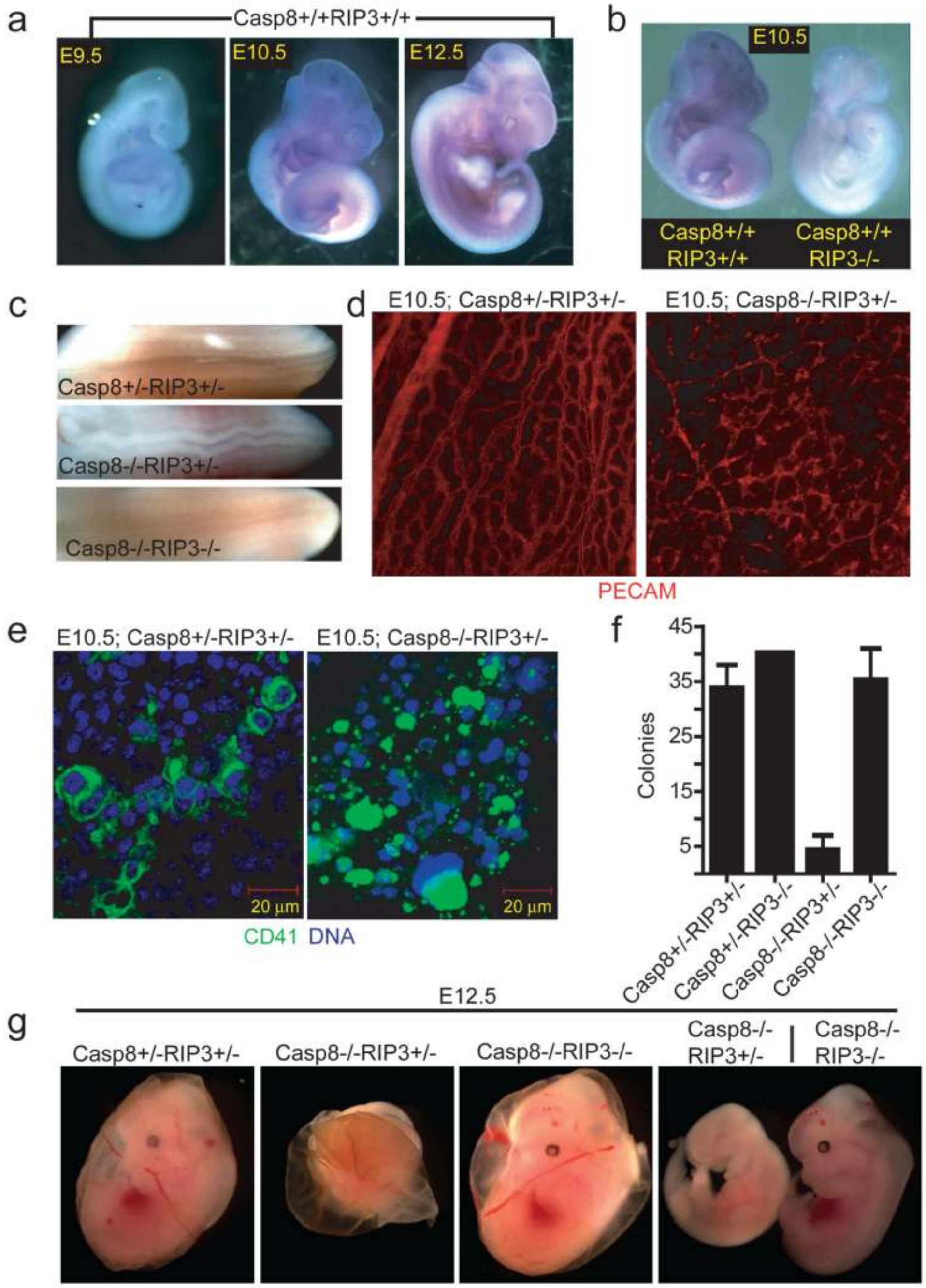

Figure 1.

Embryonic expression of *Rip3*. **(a)** Whole-mount *Rip3 in situ* hybridization of *Casp8*$^{+/+}$*Rip3*$^{+/+}$ E9.5 (left panel), E10.5 (middle panel), and E12.5 (right panel) embryos. **(b)** Whole-mount *Rip3 in situ* hybridization of *Casp8*$^{+/+}$*Rip3*$^{+/+}$ and *Casp8*$^{+/+}$*Rip3*$^{-/-}$ E10.5 embryos demonstrating specificity of the probe. **(c)** View of the neural tube of E11.5 embryos with the indicated genotype. **(d)** PECAM-1 (CD31) staining of a whole-mount E10.5 yolk sac from a representative *Casp8*$^{+/-}$*Rip3*$^{+/-}$ (left panel) and *Casp8*$^{-/-}$*Rip3*$^{+/-}$ (right panel) embryo (100X). **(e)** CD41 (green) and nuclear DNA (blue) staining of a yolk sac from a E10.5 *Casp8*$^{+/-}$*Rip3*$^{+/-}$ (left panel) and a *Casp8*$^{-/-}$*Rip3*$^{+/-}$ (right panel) embryo. **(f)** Numbers of colony-forming cells (CFC) following culture of disrupted E10.5 yolk sacs of the indicated genotype. **(g)** Photographs of E12.5 embryos and yolk sacs with the indicated genotype. The right panel shows side by side embryos with yolk sacs removed.

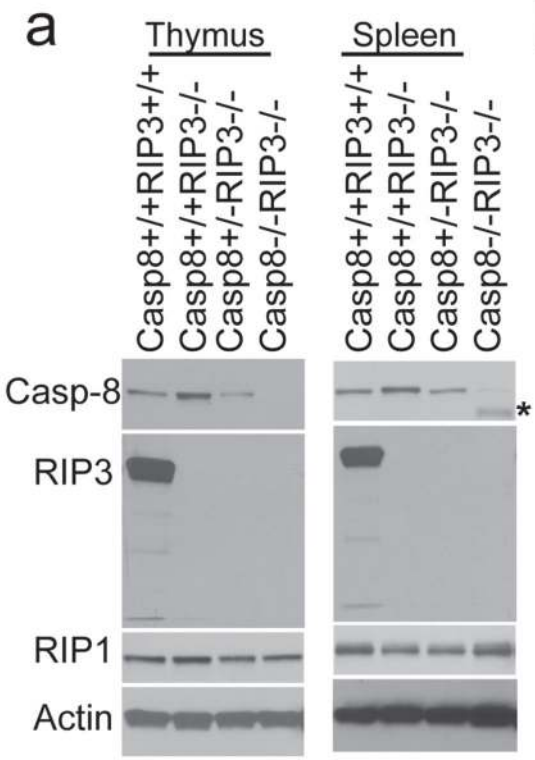

b

Genotype	Medelian Freq. (%)	Observed Freq. (%)	No. of mice
Casp8+/+RIP3+/+	6.25	6.5	8
Casp8+/+RIP3+/-	12.5	15.4	19
Casp8+/+RIP3-/-	6.25	8.1	10
Casp8+/-RIP3+/+	12.5	13.8	17
Casp8+/-RIP3+/-	25	35	43
Casp8+/-RIP3-/-	12.5	13	16
Casp8-/-RIP3+/+	6.25	0†	0†
Casp8-/-RIP3+/-	12.5	0†	0†
Casp8-/-RIP3-/-	6.25	8.1	10
†predicted embryonic lethal		total	123

Figure 2.

Casp8$^{-/-}$*Rip3*$^{-/-}$ mice are viable. **(a)** IB of Casp8, RIP3, RIP1 and β-actin from thymus (left panel) and spleen (right panel). The asterisk denotes elevated heavy IgG heavy chain reactive with secondary antibody in DKO sample. **(b)** Epistatic analysis of mice born following *Casp8*$^{+/-}$*Rip3*$^{+/-}$ intercross with predicted and observed frequencies.

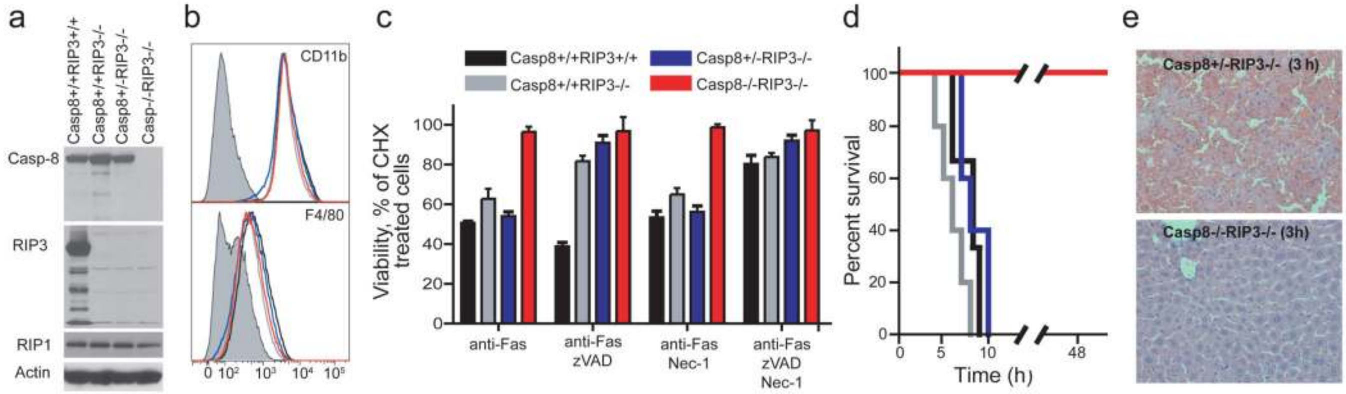

Figure 3.

Sensitivity to DR-induced apoptosis, necroptosis and disease. **(a)** IB of Casp8, RIP3, RIP1 and β-actin in BMDM derived from mice with the indicated genotype. **(b)** Relative cell surface expression levels of CD11b (top panel) or F4/80 (bottom panel) shown by red line (DKO), black line (*Casp8*$^{+/+}$*Rip3*$^{+/+}$), grey line (*Casp8*$^{+/+}$*Rip3*$^{-/-}$), or blue line (*Casp8*$^{+/-}$*Rip3*$^{-/-}$) on BMDM stained cells. Isotype control is shown by shaded histogram. **(c)** Viability of BMDM cultured in CHX (5 μg/mL) and treated with anti-Fas antibody for 18 h in the presence or absence of the caspase inhibitor zVAD-fmk (25 μM) and/or Nec-1 (30 μM). Cell viability was determined by measuring intracellular ATP levels with a Cell Titer-Glo Luminescent Cell Viability Assay kit. Error bars, SD. (n = 4). **(d)** Kaplan-Meier survival plot of 12 week old *Casp8*$^{+/+}$*Rip3*$^{+/+}$, *Casp8*$^{+/+}$*Rip3*$^{-/-}$, *Casp8*$^{+/-}$*Rip3*$^{-/-}$, and DKO mice injected intraperitoneally with 12.5 μg of anti-Fas Jo-2 antibody. Legend genotypes and line color is the same as in (c). **(e)** Histology of liver sections from *Casp8*$^{+/-}$*Rip3*$^{-/-}$ (left panel) and *Casp8*$^{-/-}$*Rip3*$^{-/-}$ mice (right panel) 3 h following injection with Jo-2 antibody.

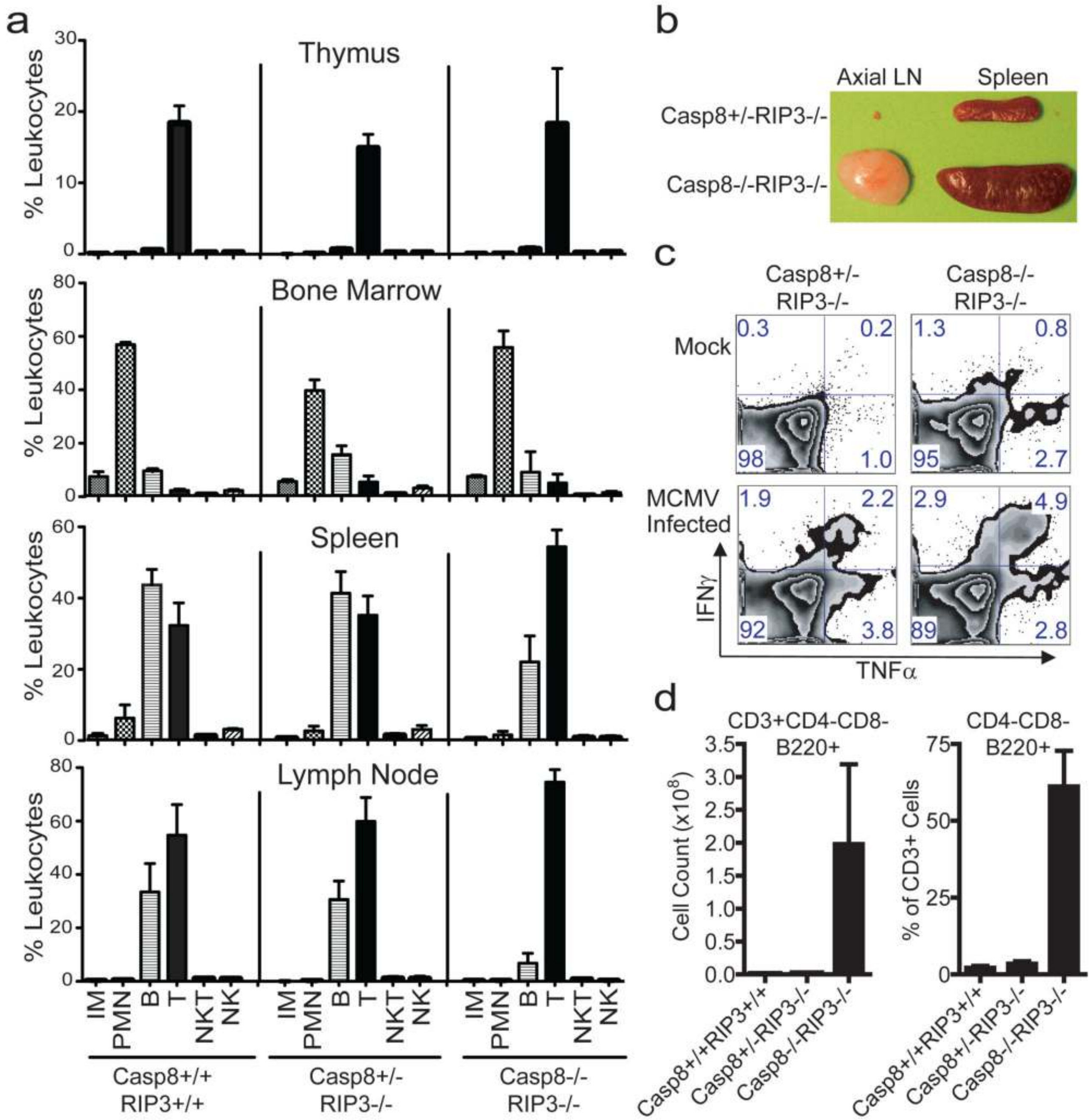

Figure 4.

Immune compartment of 16-week-old DKO mice. **(a)** Live cells from thymus (top panels), bone marrow (second set of panels), spleen (third set of panels) and LN (bottom panels), gated based on forward and side scatter properties, and stained for surface expression of CD19, CD3, CD49b, Ly6C and CD11b to define non-overlapping leukocyte ($CD45^+$) populations. The average and SD for three wild-type (left panels), four *Casp8*$^{+/-}$*RIP3*$^{-/-}$ (middle panels) littermate control and three DKO (right panels) mice showing levels of inflammatory monocytes (IM), polymorphonuclear leukocytes (PMN), B cells, T cells, NK cells and NKT cells. **(b)** Photograph of the axial LN and spleen from representative mice of the indicated genotype. **(c)** Flow cytometric analysis of IFNγ and TNFα on T cells from naïve or MCMV-infected (7 days) mice following stimulation with CD3/CD28 antibodies. $CD8^+$ T cells from one representative animal per experimental group are shown. **(d)** B220 expression was assessed on $CD4^-CD8^-$ splenic T cells. Error bars, SD.